

1 A method for genome editing in the anaerobic magnetotactic bacterium *Desulfovibrio*  
2 *magneticus* RS-1

3

4 Carly R. Grant<sup>a</sup>, Lilah Rahn-Lee<sup>a\*</sup>, Kristen N. LeGault<sup>a</sup> and Arash Komeili<sup>a#</sup>

5

6 <sup>a</sup>Department of Plant and Microbial Biology, University of California, Berkeley, CA, USA

7 #Address correspondence to Arash Komeili, [komeili@berkeley.edu](mailto:komeili@berkeley.edu)

8 \*Present address: Lilah Rahn-Lee, Department of Biology, William Jewell College,  
9 Liberty, Missouri, USA

10

11 Running Head: A genome editing method for *Desulfovibrio magneticus*

12

13 **ABSTRACT** Magnetosomes are complex bacterial organelles that serve as model  
14 systems for studying cell biology, biomineralization, and global iron cycling.  
15 Magnetosome biogenesis is primarily studied in two closely related Alphaproteobacterial  
16 *Magnetospirillum* spp. that form cubooctahedral-shaped magnetite crystals within a lipid  
17 membrane. However, chemically and structurally distinct magnetic particles have also  
18 been found in physiologically and phylogenetically diverse bacteria. Due to a lack of  
19 molecular genetic tools, the mechanistic diversity of magnetosome formation remains  
20 poorly understood. *Desulfovibrio magneticus* RS-1 is an anaerobic sulfate-reducing  
21 Deltaproteobacterium that forms bullet-shaped magnetite crystals. A recent forward  
22 genetic screen identified ten genes in the conserved magnetosome gene island of *D.*  
23 *magneticus* that are essential for its magnetic phenotype. However, this screen likely  
24 missed many interesting mutants with defects in crystal size, shape, and arrangement.

25 Reverse genetics to target the remaining putative magnetosome genes using standard  
26 genetic methods of suicide vector integration has not been feasible due to low  
27 transconjugation efficiency. Here, we present a reverse genetic method for targeted  
28 mutagenesis in *D. magneticus* using a replicative plasmid. To test this method, we  
29 generated a mutant resistant to 5-fluorouracil by making a markerless deletion of the  
30 *upp* gene that encodes uracil phosphoribosyltransferase. We also used this method for  
31 targeted marker exchange mutagenesis by replacing *kupM*, a gene identified in our  
32 previous screen as a magnetosome formation factor, with a streptomycin resistance  
33 cassette. Overall, our results show that targeted mutagenesis using a replicative  
34 plasmid is effective in *D. magneticus* and may also be applied to other genetically  
35 recalcitrant bacteria.

36 **IMPORTANCE** Magnetotactic bacteria (MTB) are a group of organisms that form small,  
37 intracellular magnetic crystals through a complex process involving lipid and protein  
38 scaffolds. These magnetic crystals and their lipid membrane, termed magnetosomes,  
39 are model systems for studying bacterial cell biology and biomineralization as well as  
40 potential platforms for biotechnological applications. Due to a lack of genetic tools and  
41 unculturable representatives, the mechanisms of magnetosome formation in  
42 phylogenetically deeply-branching MTB remain unknown. These MTB contain elongated  
43 bullet-/tooth-shaped magnetite and greigite crystals that likely form in a manner distinct  
44 from the cubooctahedral-shaped magnetite crystals of the genetically tractable  
45 Alphaproteobacteria MTB. Here, we present a method for genome editing in the  
46 anaerobic Deltaproteobacterium *Desulfovibrio magneticus* RS-1, the first cultured  
47 representative of the deeply-branching MTB. This marks a crucial step in developing *D.*

48 *magneticus* as a model for studying diverse mechanisms of magnetic particle formation  
49 by MTB.

50

51 **KEYWORDS** *Desulfovibrio*, genome editing, magnetotactic bacteria, organelles,  
52 magnetosomes, iron, biomineralization

53

## 54 **INTRODUCTION**

55 Magnetotactic bacteria (MTB) are a group of diverse microorganisms that align along  
56 magnetic fields via their intracellular chains of magnetic crystals (1, 2). Each magnetic  
57 crystal consists of either magnetite ( $\text{Fe}_3\text{O}_4$ ) or greigite ( $\text{Fe}_3\text{S}_4$ ) and is synthesized within  
58 a complex organelle called a magnetosome (3). The first cultured MTB were  
59 microaerophilic Alphaproteobacteria, which form cubooctahedral-shaped magnetite  
60 crystals, and have served as model organisms for understanding magnetosome  
61 formation (4–7). Early studies on *Magnetospirillum* spp. found a lipid-bilayer membrane,  
62 with a unique suite of proteins, surrounding each magnetite crystal (8–10). Development  
63 of genetic tools in *Magnetospirillum magneticum* AMB-1 and *Magnetospirillum*  
64 *gryphiswaldense* MSR-1 revealed a conserved magnetosome gene island (MAI) that  
65 contains the factors necessary and sufficient for the formation of the magnetosome  
66 membrane, magnetite biomineralization within the lumen of the magnetosome, and  
67 alignment of the magnetosomes in a chain along the length of the cell (3, 11). These  
68 molecular advances, along with the magnetic properties of magnetosomes, have made  
69 MTB ideal models for the study of compartmentalization and biomineralization in

70 bacteria as well as a target for the development of biomedical and industrial  
71 applications.

72

73 Improvements in isolation techniques and sequencing have revealed that MTB are  
74 ubiquitous in many aquatic environments. Based on phylogeny and magnetosome  
75 morphology, MTB can be categorized into two subgroups. The first subgroup includes  
76 members of the Proteobacteria with similar magnetosome morphology to  
77 *Magnetospirillum* spp. The second subgroup comprises MTB from more deep-branching  
78 lineages, including members of the Deltaproteobacteria, Nitrospirae, and Omnitrophica  
79 phyla, which synthesize elongated bullet-/tooth-shaped magnetite and/or greigite  
80 crystals (12, 13). While all MTB sequenced to date have their putative magnetosome  
81 genes arranged in a distinct region of their genome (3, 14–16), many of the genes  
82 essential for magnetosome biogenesis in *Magnetospirillum* spp. are missing from the  
83 genomes of deep-branching MTB (13). Likewise, a conserved set of *mad*  
84 (*magnetosome associated Deltaproteobacteria*) genes are only found in deep-branching  
85 MTB (13, 17–19). This suggests a genetic diversity underpinning the control of  
86 magnetosome morphology and physiology in non-model MTB that is distinct from the  
87 well-characterized *Magnetospirillum* spp.

88

89 *Desulfovibrio magneticus* RS-1, the first cultured MTB outside of the  
90 Alphaproteobacteria, is an anaerobic sulfate-reducing Deltaproteobacterium that forms  
91 irregular bullet-shaped crystals of magnetite (20, 21). As with the *Magnetospirillum* spp.,  
92 the magnetosome genes of *D. magneticus* are located within a MAI and include

93 homologs to some *mam* genes as well as *mad* genes (13, 17, 22). Recently, we used a  
94 forward genetic screen combining random chemical and UV mutagenesis with whole  
95 genome resequencing to identify mutations in ten *mam* and *mad* genes of the *D.*  
96 *magneticus* MAI that resulted in non-magnetic phenotypes (19). However, this screen  
97 relied on a strict selection scheme for nonmagnetic mutants. As such, we likely missed  
98 magnetosome genes that are important for regulating the shape, size, and arrangement  
99 of magnetosomes. In order to elucidate the degree of conservation between *mam*  
100 genes and determine a function for the *mad* genes in *D. magneticus*, a reverse genetic  
101 method for targeted mutagenesis is necessary.

102

103 *Desulfovibrio* spp. have gained much attention for their important roles in the global  
104 cycling of numerous elements, in biocorrosion, and in the bioremediation of toxic metal  
105 ions (23, 24). Development of genetic tools, such as expression vectors, transposons,  
106 and targeted genome editing systems, has allowed for a more detailed examination of  
107 the important activities of a few *Desulfovibrio* spp. (25, 26). Targeted mutagenesis using  
108 a one-step double recombination method was first achieved in *Desulfovibrio*  
109 *fructosovorans* and, more recently, in *Desulfovibrio gigas* and *Desulfovibrio*  
110 *desulfuricans* ND132 (27–29). In this method, plasmids that are electroporated into the  
111 cell are thought to be rapidly linearized by endogenous restriction-modification systems  
112 (29–31). The linearized plasmid DNA, carrying a selectable marker flanked by upstream  
113 and downstream regions of homology to a target gene, can then undergo double  
114 recombination into the chromosome in one step (**Fig. 1A**). This efficient one-step  
115 method, which is dependent on electroporation of the plasmid (27–29), is unlikely to be

116 applicable in *D. magneticus* because plasmid uptake has only been demonstrated using  
117 conjugal transfer (19). The second targeted mutagenesis method, used in *Desulfovibrio*  
118 *vulgaris* Hildenborough, is a two-step double recombination that makes use of a non-  
119 replicative, or suicide, vector (30, 31). In the first step of this method, a suicide vector,  
120 with sequences upstream and downstream of the target gene, integrates into the  
121 genome upon the first homologous recombination event (**Fig. 1B**). Next, a second  
122 recombination event occurs whereby the vector is excised from the genome and cells  
123 with the desired genotype are selected with an antibiotic marker and/or a  
124 counterselection marker (30, 31) (**Fig. 1B**). For many bacteria, including *D. magneticus*,  
125 plasmid uptake and integration occur at low enough frequencies to prevent the use of  
126 suicide vectors for genetic manipulation (19).

127  
128 Here, we develop a method for targeted gene deletion using a replicative plasmid,  
129 thereby bypassing the need for suicide vector integration (**Fig. 1C**). We generated a  
130 mutant resistant to 5-fluorouracil by making a markerless deletion of the *upp* gene which  
131 encodes an enzyme in the pyrimidine salvage pathway that is nonessential under  
132 standard laboratory conditions. Additionally, we deleted *kupM*, a gene encoding a  
133 potassium transporter that acts as a magnetosome formation factor (19), via marker  
134 exchange with a streptomycin resistance cassette. Deletion of both *upp* and *kupM*  
135 conferred the expected phenotypes, which were subsequently complemented *in trans*.  
136 Overall, our results show that targeted mutagenesis using a replicative plasmid is  
137 possible in *D. magneticus*. It may also be suitable for other bacteria for which replicative  
138 plasmid uptake is possible, but at a rate too low for suicide vector integration.

139

## 140 RESULTS

141 **Design of a replicative deletion plasmid using *sacB* counterselection.** Targeted  
142 genetic manipulation in most bacteria requires a method to efficiently deliver foreign  
143 DNA destined for integration into the chromosome. One commonly used method  
144 involves suicide vector uptake and integration prior to the first selection step (**Fig. 1B**).  
145 In *D. magneticus*, plasmid transfer has only been achieved via conjugation at low  
146 efficiencies making the uptake and subsequent integration of suicide vectors into its  
147 chromosome an unlikely event (19). As such, we hypothesized that we could bypass the  
148 need for a suicide vector by using a stable, replicative plasmid designed to delete  
149 specific genes via homologous recombination (**Fig. 1C**). Two features of this method  
150 will allow for isolation of desired mutants: (1) a selectable marker is used to identify  
151 double recombination events at the targeted site and (2) a counterselectable marker  
152 distinguishes the desired mutant cells, which have lost all remaining copies of the  
153 plasmid.

154

155 *sacB* is a common counterselection marker that is effective in many bacteria. The *sacB*  
156 gene from *Bacillus subtilis* encodes levansucrase, which converts sucrose to levans that  
157 are lethal to many Gram-negative bacteria, including *D. vulgaris* Hildenborough (30, 32,  
158 33). To test its functionality in *D. magneticus*, we inserted *sacB* under the expression of  
159 the *mamA* promoter in a plasmid that replicates in both *Escherichia coli* and *D.*  
160 *magneticus* (**Fig. 2A**). This plasmid (pAK914) and a control plasmid were then  
161 conjugated into *D. magneticus*. We found no growth inhibition for *D. magneticus* cells

162 with the control plasmid in the presence of sucrose and kanamycin. In contrast, cells  
163 expressing *sacB* were unable to grow with kanamycin and sucrose concentrations of  
164 1% (w/v) or higher (data not shown). To test if plasmids could be cured, *D. magneticus*  
165 with pAK914 was passaged two times in liquid media containing no antibiotic and plated  
166 on 1% sucrose. Individual sucrose resistant ( $\text{Suc}^r$ ) colonies were inoculated and  
167 screened for kanamycin sensitivity ( $\text{Kan}^s$ ). All isolated colonies (n=16) were  $\text{Kan}^s$ ,  
168 suggesting that the cells had lost the plasmid. These experiments demonstrate that  
169 *sacB* is a suitable counterselection marker in *D. magneticus*.

170  
171 **Construction of a  $\Delta upp$  strain by markerless deletion.** To test our replicative  
172 deletion method, we chose to target the *upp* gene, the mutation of which has a  
173 selectable phenotype. The *upp* gene encodes uracil phosphoribosyltransferase  
174 (UPRTase), a key enzyme in the pyrimidine salvage pathway that catalyzes the reaction  
175 of uracil with 5-phosphoribosyl- $\alpha$ -1-pyrophosphate (PRPP) to UMP and  $\text{PP}_i$  (34) (**Fig.**  
176 **3A**). When given the pyrimidine analog 5-fluorouracil (5-FU), UPRTase catalyzes the  
177 production of 5-fluoroxypyridine monophosphate (5-FUMP). 5-FUMP is further  
178 metabolized and incorporated into DNA, RNA, and sugar nucleotides resulting in  
179 eventual cell death (**Fig. 3A**) (35, 36). Previous studies have shown that  $\Delta upp$  mutants  
180 of *D. vulgaris* Hildenborough are resistant to 5-FU while wild type (WT) cells are  
181 effectively killed by the pyrimidine analog (31, 37). The *D. magneticus* genome has a  
182 homolog (*DMR\_08390*) to the *D. vulgaris* Hildenborough *upp* gene that is likely  
183 functional as detected by the sensitivity of *D. magneticus* to 5-FU (**Fig. 3B**, **Fig. 4A**). To  
184 show that the *upp* gene product confers 5-FU sensitivity and to validate our replicative



185 deletion system, we chose to target the *D. magneticus upp* gene for markerless  
186 deletion.

187  
188 To construct a *upp* deletion vector, a markerless cassette containing the regions  
189 upstream and downstream of the *upp* gene were inserted into plasmid pAK914 (**Fig.**  
190 **2B**). The resulting plasmid (pAK1126) was transferred to WT *D. magneticus* and a non-  
191 magnetic strain ( $\Delta$ MAI) (19) by conjugation and single, kanamycin resistant (Kan<sup>r</sup>)  
192 colonies were isolated and passaged in growth medium containing no antibiotic. After  
193 the third passage, *upp* mutants that had lost the vector backbone were selected for with  
194 5-FU and sucrose. Compared with a control plasmid (pAK914), over 10-fold more 5-FU  
195 resistant (5-FU<sup>r</sup>) mutants were obtained from pAK1126. PCR of the region flanking the  
196 *upp* gene confirmed that the 5-FU<sup>r</sup> colonies from pAK1126 resulted in markerless  
197 deletion of *upp* ( $\Delta$ *upp*) while 5-FU<sup>r</sup> colonies from pAK914 were likely the result of point  
198 mutations (**Fig. 3B, Fig. 3D**). Similar to results obtained for *D. vulgaris* Hildenborough  
199 (31), the  $\Delta$ *upp* mutant of *D. magneticus* was able to grow in the presence of 5-FU (**Fig.**  
200 **4B, Table 2**). Complementation of the *upp* gene *in trans* restored UPRTase function  
201 and cells were no longer able to grow with 5-FU (**Fig. 2C, Fig. 4C, Table 2**). These  
202 experiments demonstrate that a replicative plasmid can be used to directly edit the *D.*  
203 *magneticus* genome.

204  
205 **Construction of a  $\Delta$ *kup* strain by marker exchange mutagenesis.** Because many  
206 genetic mutations confer no selectable phenotype, we sought to develop our replicative  
207 deletion plasmid for marker exchange mutagenesis. To test this system, we chose to

208 replace a gene with a known phenotype, *kupM* (*DMR\_40800*), with a streptomycin-  
209 resistance gene cassette (*strAB*). *kupM* is located in the *D. magneticus* MAI and  
210 encodes a functional potassium transporter (19). Mutant alleles in *kupM*, including  
211 missense, nonsense, and frameshift mutations, were previously identified in our screen  
212 for non-magnetic mutants (19). These *kupM* mutations resulted in cells that rarely  
213 contained electron-dense particles and were unable to turn in a magnetic field, as  
214 measured by the coefficient of magnetism or  $C_{mag}$  (19).

215  
216 To mutate *kupM*, we inserted a marker-exchange cassette, with regions upstream and  
217 downstream of *kupM* flanking *strAB*, into pAK914 (**Fig. 2D**) to create the deletion  
218 plasmid pAK941. Following conjugation, single colonies of *D. magneticus* with pAK941  
219 were isolated by kanamycin selection. After three passages in growth medium without  
220 selection, potential mutants were isolated on plates containing streptomycin and  
221 sucrose. Single colonies (n=48) that were streptomycin resistant ( $Str^r$ ) and  $Suc^r$  were  
222 inoculated into liquid medium and screened for  $Kan^s$ . Of the ten isolates that were  $Kan^s$ ,  
223 two had the correct genotype ( $\Delta kupM::strAB$ ) as confirmed by PCR and sequencing  
224 (**Fig. 3C, Fig. 3E**).

225  
226 Similar to the phenotypes previously observed in *kupM* mutants (19),  $\Delta kupM::strAB$   
227 cells were severely defective in magnetosome synthesis and ability to turn in a magnetic  
228 field (**Fig. 5**). Though a slight  $C_{mag}$  could be measured, few cells contained electron-  
229 dense particles or magnetosomes. Importantly, the WT phenotype was rescued by  
230 expressing *kupM* on a plasmid in the  $\Delta kupM::strAB$  mutant (**Fig. 5**). These results

231 confirm that the replicative deletion plasmid method described here can be used  
232 successfully for marker exchange mutagenesis.

233

## 234 **DISCUSSION**

235 In this study, we expand the genetic toolbox of *D. magneticus* to include a replicative  
236 plasmid method for targeted mutagenesis (**Fig. 1C**). We show the utility of this method  
237 for markerless deletion of genes with a selectable phenotype and for marker exchange  
238 mutagenesis. Some of the earliest examples of targeted mutagenesis in Gram-negative  
239 bacteria used replicative plasmids, similar to the method described here. (33, 38).  
240 These studies, which predated the application of suicide vectors, relied on plasmid  
241 instability by introducing a second plasmid of the same incompatibility group or by  
242 limiting nutrients in the growth medium (33, 38).

243

244 Because the *D. magneticus* genetic toolbox has a limited number of plasmids, antibiotic  
245 markers, and narrow growth constraints, we used a replicative plasmid and established  
246 *sacB* as a counterselection marker to generate and isolate mutants. While *sacB*  
247 counterselection was ultimately successful, a large number of false-positives were also  
248 isolated at the sucrose selection step. Mutations in *sacB* have been found to occur at a  
249 high frequency in many bacteria (30, 39–42). Indeed, we found that deletions and  
250 mutations in *P<sub>mamA</sub>\_sacB* are abundant in the false-positive Suc<sup>r</sup> Str<sup>r</sup> isolates (data not  
251 shown). Alternative counterselection markers, including *upp*, have been shown to select  
252 for fewer false-positives (31, 42–44). Since *D. magneticus* is sensitive to 5-FU only  
253 when the *upp* gene is present (**Fig. 4**), the *upp* mutants generated in this study may be

254 used as the parent strains for future targeted mutagenesis using *upp* as a  
255 counterselectable marker rather than *sacB*. Additionally, the combined use of *upp* and  
256 *sacB* for counterselection could reduce the false-positive background that results from  
257 the accumulation of mutations in these markers.

258

259 The replicative deletion plasmid described here is designed to replace a target gene  
260 with an antibiotic resistance marker. As such, the construction of strains with multiple  
261 directed mutations will be complicated by the need for additional antibiotic-resistance  
262 markers, which are limited in *D. magneticus*. These limitations may be overcome by  
263 removing the chromosomal antibiotic marker in subsequent steps (33, 45, 46).  
264 Ultimately, improvements in conjugation efficiency or methods for electroporation with  
265 high transformation efficiency are desired. Similar to the ongoing development of  
266 genetics in *D. vulgaris* Hildenborough, establishment of a suicide vector delivery system  
267 in *D. magneticus* will allow for more high-throughput targeted mutagenesis and even the  
268 construction of markerless deletion mutants (25, 31).

269

270 Overall, we have demonstrated the utility of a replicative deletion plasmid used to  
271 generate the first targeted mutants of *D. magneticus*. This method marks a crucial step  
272 in developing *D. magneticus* as a model for the study of anaerobic sulfate reduction and  
273 diverse mechanisms of magnetic particle formation by MTB. Both MTB and sulfate-  
274 reducing bacteria have been singled out for their role in the global cycling of numerous  
275 elements and for potential applications, such as bioremediation (23, 24, 47, 48). *D.*  
276 *magneticus*, in particular, may be useful in the bioremediation of heavy-metals and in

277 the global cycling of iron, since it can form both magnetosomes and other iron-  
278 containing organelles (49, 50). Through genetic manipulation of *D. magneticus*,  
279 pathways of elemental cycling and heavy-metal turnover may now be explored.  
280 Additionally, genetic manipulation of *D. magneticus* will further our understanding of  
281 magnetosome formation and provide answers to many longstanding questions for the  
282 deeply-branching MTB: Which proteins regulate and control magnetosome formation?  
283 To what extent are lipid membranes involved in forming these crystals? How is the  
284 elongated and irregular crystal shape achieved? Finally, in addition to *D. magneticus*,  
285 the method described here may extend to other bacteria that are not amenable to  
286 targeted mutagenesis with suicide vectors but are able to accommodate replicative  
287 plasmids.

288

## 289 **MATERIALS AND METHODS**

290 **Strains, media, and growth conditions.** The bacterial strains used in this study are  
291 listed in Table 1. All *E. coli* strains were cultured aerobically with continuous shaking at  
292 250 RPM at 37°C in lysogeny broth (LB). *D. magneticus* strains were grown  
293 anaerobically at 30°C in sealed Balch tubes with a N<sub>2</sub> headspace containing RS-1  
294 Growth Medium (RGM) that was degassed with N<sub>2</sub>, unless otherwise stated (50).  
295 Sodium pyruvate (10 mM) was used as an electron donor with fumaric acid disodium  
296 (10 mM) as the terminal electron acceptor. RGM was buffered with Hepes and the pH  
297 was adjusted to 6.7 with NaOH (19). Before inoculating with cells, RGM was  
298 supplemented with 0.8% (v/v) Wolfe's vitamins, 100 μM ferric malate, and 285 μM  
299 cysteine-HCl (50). Solid agar plates were prepared by adding 1.5% agar (wt/vol) to LB

300 and 1% agar (wt/vol) to RGM. Vitamins (0.8% v/v), ferric malate (20  $\mu$ M), and cysteine  
301 (285  $\mu$ M) were added to the molten RGM agar, as well as antibiotics and selective  
302 agents, as needed. For *D. magneticus*, all plating steps were carried out aerobically,  
303 transferred to an anaerobic jar, and incubated at 30°C for 10-14 days, as described  
304 previously (19). Antibiotics and selective agents used are as follows: kanamycin (50  
305  $\mu$ g/mL for *E. coli* strains, 125  $\mu$ g/ml for *D. magneticus* strains), streptomycin (50  $\mu$ g/ml  
306 for *E. coli* and *D. magneticus* strains), diaminopimelic acid (300  $\mu$ M for *E. coli* WM3064),  
307 5-FU (2.5  $\mu$ g/ml for *D. magneticus* strains), and sucrose (1% for *D. magneticus* strains).

308

309 **Plasmids and cloning.** All plasmids used in this work are listed in Table 1. All cloning  
310 was performed in *E. coli* DH5 $\alpha$   $\lambda$ pir using the Gibson method or restriction enzyme  
311 ligation (Gibson, et al 2009). For PCR amplification, KOD (EMD Millipore, Germany)  
312 and GoTaq (Promega, USA) DNA polymerases were used with the primers listed in  
313 Table S1. All upstream and downstream homology regions were amplified from *D.*  
314 *magneticus* genomic DNA. *strAB* and *P<sub>npT</sub>* were amplified from pBMS6 and pLR6,  
315 respectively, and subcloned into pBMC7 to make pAK920 which served as the template  
316 for amplifying *P<sub>npT</sub>-strAB* for the deletion vectors. *sacB* was amplified from pAK0 and  
317 inserted into pLR6 digested with Sall and XbaI to create pAK914. To construct a  
318 plasmid for the targeted deletion of *upp* (*DMR\_08390*), 991 bp upstream and 1012 bp  
319 downstream of *upp* were amplified and inserted into pAK914 digested with XbaI and  
320 SacI using a 3-piece Gibson assembly. To create the *upp* complementation plasmid,  
321 pAK914 was digested with BamHI and SacI and the *upp* gene, with its promoter, were  
322 PCR amplified from *D. magneticus* genomic DNA. To construct pAK941 for marker

323 exchange mutagenesis of *kupM*, a cassette of 1064 bp upstream region and 1057 bp  
324 downstream region flanking *P<sub>npt</sub>\_strAB* was assembled using Gibson cloning. The  
325 cassette was amplified and inserted into pAK914 digested with XbaI using a two-piece  
326 Gibson assembly.

327

328 ***upp* and *kup* mutant generation and complementation.** Replicative deletion  
329 plasmids were transformed into *E. coli* WM3064 by heat shock and transferred to *D.*  
330 *magneticus* by conjugation, as described previously (19). Single colonies of Kan<sup>r</sup> *D.*  
331 *magneticus* were isolated and inoculated into RGM containing no antibiotic. Cultures  
332 were passaged three times and spread on 1% agar RGM plates containing either 50  
333 µg/ml streptomycin and 1% sucrose or 2.5 µg/ml 5-FU and 1% sucrose. Single colonies  
334 were screened for Kan<sup>s</sup> and by PCR using the primers listed in Table 2. Successful *upp*  
335 and *kup* mutants were confirmed by Sanger sequencing. Expression plasmids for the  
336 complementation of  $\Delta kup::strAB$  and  $\Delta upp$  as well as empty vectors for controls were  
337 transferred to *D. magneticus* strains as described above. Transconjugants were  
338 inoculated into RGM containing kanamycin in order to maintain the plasmids.

339

340 **Mutant phenotype and complementation analyses.** The growth and coefficient of  
341 magnetism ( $C_{mag}$ ) of *D. magneticus* strains were measured in a Spec20  
342 spectrophotometer at an optical density of 650 nm ( $OD_{650}$ ), as described previously (10,  
343 50). For *upp* mutant and complementation analysis, RGM was supplemented with 5-FU  
344 (2.5 µg/ml in 0.1% DMSO) or DMSO (0.1%) and growth was measured for WT and  
345  $\Delta upp$  strains with an empty vector (pAK914) and for the  $\Delta upp$  strain with the

346 complementation plasmid pAK1127. For *kup* mutant and complementation analysis, the  
347  $C_{\text{mag}}$  was measured by placing a large bar magnet parallel or perpendicular to the  
348 sample in order to measure the maximum or minimum absorbance, respectively, as the  
349 *D. magneticus* strains rotate 90 degrees with the magnetic field. The ratio of maximum  
350 to minimum absorbances was calculated as the  $C_{\text{mag}}$  (10). Whole-cell transmission  
351 electron microscopy (TEM) was performed as previously described (50). The  $C_{\text{mag}}$   
352 calculations and TEM were performed for WT *D. magneticus* with an empty vector  
353 (pBMK7) and  $\Delta\text{kup}::\text{strAB}$  with an empty vector (pBMK7) or complementation plasmid  
354 (pLR41). For all growth measurements,  $C_{\text{mag}}$  measurements, and TEM, plasmids were  
355 maintained in cells with 125  $\mu\text{g}/\text{ml}$  kanamycin.

356

## 357 **ACKNOWLEDGMENTS**

358 We would like to thank the members of the Komeili lab for helpful suggestions and  
359 discussions and the staff at the University of California Berkeley Electron Microscope  
360 Laboratory for advice and assistance in electron microscopy sample preparation and  
361 data collection.

362

## 363 **FUNDING INFORMATION**

364 This work was supported by grants from the National Institutes of Health  
365 (R01GM084122 and R35GM127114), the National Science Foundation (1504681) and  
366 the Office of Naval Research (N000141310421).

367

## 368 **REFERENCES**



- 369 1. Bellini S. 2009. On a unique behavior of freshwater bacteria. *Chin J Oceanol*  
370 *Limnol* 27:3.
- 371 2. Blakemore R. 1975. Magnetotactic bacteria. *Science* 190:377–379.
- 372 3. Uebe R, Schüler D. 2016. Magnetosome biogenesis in magnetotactic bacteria. *Nat*  
373 *Rev Microbiol* 14:621–637.
- 374 4. Bazylinski DA, Frankel RB, Jannasch HW. 1988. Anaerobic magnetite production  
375 by a marine, magnetotactic bacterium. *Nature* 334:518–519.
- 376 5. Blakemore RP, Maratea D, Wolfe RS. 1979. Isolation and pure culture of a  
377 freshwater magnetic spirillum in chemically defined medium. *J Bacteriol* 140:720–  
378 729.
- 379 6. Matsunaga T, Sakaguchi T, Tadakoro F. 1991. Magnetite formation by a magnetic  
380 bacterium capable of growing aerobically. *Appl Microbiol Biotechnol* 35:651–655.
- 381 7. Schüler D, Köhler M. 1992. The isolation of a new magnetic spirillum. *Zentralblatt*  
382 *Für Mikrobiol* 147:150–151.
- 383 8. Balkwill DL, Maratea D, Blakemore RP. 1980. Ultrastructure of a magnetotactic  
384 spirillum. *J Bacteriol* 141:1399–1408.
- 385 9. Gorby YA, Beveridge TJ, Blakemore RP. 1988. Characterization of the bacterial  
386 magnetosome membrane. *J Bacteriol* 170:834–841.
- 387 10. Komeili A, Vali H, Beveridge TJ, Newman DK. 2004. Magnetosome vesicles are  
388 present before magnetite formation, and MamA is required for their activation. *Proc*  
389 *Natl Acad Sci U S A* 101:3839–3844.
- 390 11. Komeili A. 2012. Molecular mechanisms of compartmentalization and  
391 biomineralization in magnetotactic bacteria. *FEMS Microbiol Rev* 36:232–255.

- 392 12. Lefèvre CT, Bazylinski DA. 2013. Ecology, Diversity, and Evolution of  
393 Magnetotactic Bacteria. *Microbiol Mol Biol Rev* 77:497–526.
- 394 13. Lin W, Zhang W, Zhao X, Roberts AP, Paterson GA, Bazylinski DA, Pan Y. 2018.  
395 Genomic expansion of magnetotactic bacteria reveals an early common origin of  
396 magnetotaxis with lineage-specific evolution. *ISME J* 12:1508–1519.
- 397 14. Kolinko I, Lohße A, Borg S, Raschdorf O, Jogler C, Tu Q, Pósfai M, Tompa É,  
398 Plitzko JM, Brachmann A, Wanner G, Müller R, Zhang Y, Schüler D. 2014.  
399 Biosynthesis of magnetic nanostructures in a foreign organism by transfer of  
400 bacterial magnetosome gene clusters. *Nat Nanotechnol* 9:193–197.
- 401 15. Murat D, Quinlan A, Vali H, Komeili A. 2010. Comprehensive genetic dissection of  
402 the magnetosome gene island reveals the step-wise assembly of a prokaryotic  
403 organelle. *Proc Natl Acad Sci U S A* 107:5593–5598.
- 404 16. Murat D, Falahati V, Bertinetti L, Csencsits R, Körnig A, Downing K, Faivre D,  
405 Komeili A. 2012. The magnetosome membrane protein, MmsF, is a major regulator  
406 of magnetite biomineralization in *Magnetospirillum magneticum* AMB-1. *Mol*  
407 *Microbiol* 85:684–699.
- 408 17. Lefèvre CT, Trubitsyn D, Abreu F, Kolinko S, Jogler C, de Almeida LGP, de  
409 Vasconcelos ATR, Kube M, Reinhardt R, Lins U, Pignol D, Schüler D, Bazylinski  
410 DA, Ginet N. 2013. Comparative genomic analysis of magnetotactic bacteria from  
411 the Deltaproteobacteria provides new insights into magnetite and greigite  
412 magnetosome genes required for magnetotaxis. *Environ Microbiol* 15:2712–2735.

- 413 18. Lin W, Deng A, Wang Z, Li Y, Wen T, Wu L-F, Wu M, Pan Y. 2014. Genomic  
414 insights into the uncultured genus '*Candidatus Magnetobacterium*' in the phylum  
415 *Nitrospirae*. ISME J 8:2463–2477.
- 416 19. Rahn-Lee L, Byrne ME, Zhang M, Sage DL, Glenn DR, Milbourne T, Walsworth  
417 RL, Vali H, Komeili A. 2015. A Genetic Strategy for Probing the Functional Diversity  
418 of Magnetosome Formation. PLOS Genet 11:e1004811.
- 419 20. Sakaguchi T, Arakaki A, Matsunaga T. 2002. *Desulfovibrio magneticus* sp. nov., a  
420 novel sulfate-reducing bacterium that produces intracellular single-domain-sized  
421 magnetite particles. Int J Syst Evol Microbiol 52:215–221.
- 422 21. Sakaguchi T, Burgess JG, Matsunaga T. 1993. Magnetite formation by a sulphate-  
423 reducing bacterium. Nature 365:47–49.
- 424 22. Nakazawa H, Arakaki A, Narita-Yamada S, Yashiro I, Jinno K, Aoki N, Tsuruyama  
425 A, Okamura Y, Tanikawa S, Fujita N, Takeyama H, Matsunaga T. 2009. Whole  
426 genome sequence of *Desulfovibrio magneticus* strain RS-1 revealed common gene  
427 clusters in magnetotactic bacteria. Genome Res 19:1801–1808.
- 428 23. Barton LL, Fauque GD. 2009. Chapter 2 Biochemistry, Physiology and  
429 Biotechnology of Sulfate-Reducing Bacteria, p. 41–98. *In* Advances in Applied  
430 Microbiology. Academic Press.
- 431 24. Heidelberg JF, Seshadri R, Haveman SA, Hemme CL, Paulsen IT, Kolonay JF,  
432 Eisen JA, Ward N, Methe B, Brinkac LM, Daugherty SC, Deboy RT, Dodson RJ,  
433 Durkin AS, Madupu R, Nelson WC, Sullivan SA, Fouts D, Haft DH, Selengut J,  
434 Peterson JD, Davidsen TM, Zafar N, Zhou L, Radune D, Dimitrov G, Hance M,  
435 Tran K, Khouri H, Gill J, Utterback TR, Feldblyum TV, Wall JD, Voordouw G,

- 436 Fraser CM. 2004. The genome sequence of the anaerobic, sulfate-reducing  
437 bacterium *Desulfovibrio vulgaris* Hildenborough. *Nat Biotechnol* 22:554–559.
- 438 25. Keller KL, Wall JD. 2011. Genetics and Molecular Biology of the Electron Flow for  
439 Sulfate Respiration in *Desulfovibrio*. *Front Microbiol* 2.
- 440 26. Wall JD, Hemme CL, Rapp-Giles B, Ringbauer JA, Casalot L, Giblin T. 2003.  
441 Genes and Genetic Manipulations of *Desulfovibrio*, p. 85–98. *In* *Biochemistry and*  
442 *Physiology of Anaerobic Bacteria*. Springer, New York, NY.
- 443 27. Broco Manuela, Rousset Marc, Oliveira Solange, Rodrigues-Pousada Claudina.  
444 2005. Deletion of flavoredoxin gene in *Desulfovibrio gigas* reveals its participation  
445 in thiosulfate reduction. *FEBS Lett* 579:4803–4807.
- 446 28. Parks JM, Johs A, Podar M, Bridou R, Hurt RA, Smith SD, Tomanicek SJ, Qian Y,  
447 Brown SD, Brandt CC, Palumbo AV, Smith JC, Wall JD, Elias DA, Liang L. 2013.  
448 The Genetic Basis for Bacterial Mercury Methylation. *Science* 339:1332–1335.
- 449 29. Rousset M, Dermoun Z, Chippaux M, Bélaich JP. 1991. Marker exchange  
450 mutagenesis of the *hydN* genes in *Desulfovibrio fructosovorans*. *Mol Microbiol*  
451 5:1735–1740.
- 452 30. Fu R, Voordouw G. 1997. Targeted gene-replacement mutagenesis of *dcrA*,  
453 encoding an oxygen sensor of the sulfate-reducing bacterium *Desulfovibrio vulgaris*  
454 Hildenborough. *Microbiology* 143:1815–1826.
- 455 31. Keller KL, Bender KS, Wall JD. 2009. Development of a Markerless Genetic  
456 Exchange System for *Desulfovibrio vulgaris* Hildenborough and Its Use in  
457 Generating a Strain with Increased Transformation Efficiency. *Appl Environ*  
458 *Microbiol* 75:7682–7691.

- 459 32. Gay P, Coq DL, Steinmetz M, Ferrari E, Hoch JA. 1983. Cloning structural gene  
460 *sacB*, which codes for exoenzyme levansucrase of *Bacillus subtilis*: expression of  
461 the gene in *Escherichia coli*. J Bacteriol 153:1424–1431.
- 462 33. Ried JL, Collmer A. 1987. An *nptI-sacB-sacR* cartridge for constructing directed,  
463 unmarked mutations in Gram-negative bacteria by marker exchange- eviction  
464 mutagenesis. Gene 57:239–246.
- 465 34. Neuhard J. 1983. Utilization of preformed pyrimidine bases and nucleosides /  
466 Utilization of preformed pyrimidine bases and nucleosides, p. 95–148. In  
467 Metabolism of nucleotides, nucleosides and nucleobases in microorganisms /  
468 edited by A. Munch-Petersen. Academic Press, New York, NY.
- 469 35. Singh V, Brecik M, Mukherjee R, Evans JC, Svetlíková Z, Blaško J, Surade S,  
470 Blackburn J, Warner DF, Mikušová K, Mizrahi V. 2015. The Complex Mechanism  
471 of Antimycobacterial Action of 5-Fluorouracil. Chem Biol 22:63–75.
- 472 36. Cohen SS, Flaks JG, Barner HD, Loeb MR, Lichtenstein J. 1958. The mode of  
473 action of 5-fluorouracil and its derivatives. Proc Natl Acad Sci U S A 44:1004–1012.
- 474 37. Bender KS, Cheyen H, Wall JD. 2006. Analysing the Metabolic Capabilities of  
475 *Desulfovibrio* Species through Genetic Manipulation. Biotechnol Genet Eng Rev  
476 23:157–174.
- 477 38. Ruvkun GB, Ausubel FM. 1981. A general method for site-directed mutagenesis in  
478 prokaryotes. Nature 289:85–88.
- 479 39. Bloor AE, Cranenburgh RM. 2006. An Efficient Method of Selectable Marker Gene  
480 Excision by Xer Recombination for Gene Replacement in Bacterial Chromosomes.  
481 Appl Environ Microbiol 72:2520–2525.

- 482 40. Cai YP, Wolk CP. 1990. Use of a conditionally lethal gene in *Anabaena* sp. strain  
483 PCC 7120 to select for double recombinants and to entrap insertion sequences. *J*  
484 *Bacteriol* 172:3138–3145.
- 485 41. Kaniga K, Delor I, Cornelis GR. 1991. A wide-host-range suicide vector for  
486 improving reverse genetics in Gram-negative bacteria: inactivation of the *blaA* gene  
487 of *Yersinia enterocolitica*. *Gene* 109:137–141.
- 488 42. Ma W, Wang X, Mao Y, Wang Z, Chen T, Zhao X. 2015. Development of a  
489 markerless gene replacement system in *Corynebacterium glutamicum* using *upp*  
490 as a counter-selection marker. *Biotechnol Lett* 37:609–617.
- 491 43. Graf N, Altenbuchner J. 2011. Development of a Method for Markerless Gene  
492 Deletion in *Pseudomonas putida*. *Appl Environ Microbiol* 77:5549–5552.
- 493 44. Wang Y, Zhang C, Gong T, Zuo Z, Zhao F, Fan X, Yang C, Song C. 2015. An *upp*-  
494 based markerless gene replacement method for genome reduction and metabolic  
495 pathway engineering in *Pseudomonas mendocina* NK-01 and *Pseudomonas putida*  
496 KT2440. *J Microbiol Methods* 113:27–33.
- 497 45. Fabret C, Dusko Ehrlich S, Noirot P. 2002. A new mutation delivery system for  
498 genome-scale approaches in *Bacillus subtilis*. *Mol Microbiol* 46:25–36.
- 499 46. Huang LC, Wood EA, Cox MM. 1997. Convenient and reversible site-specific  
500 targeting of exogenous DNA into a bacterial chromosome by use of the FLP  
501 recombinase: the FLIRT system. *J Bacteriol* 179:6076–6083.
- 502 47. Chen AP, Berounsky VM, Chan MK, Blackford MG, Cady C, Moskowitz BM, Kraal  
503 P, Lima EA, Kopp RE, Lumpkin GR, Weiss BP, Hesse P, Vella NGF. 2014.

- 504 Magnetic properties of uncultivated magnetotactic bacteria and their contribution to  
505 a stratified estuary iron cycle. *Nat Commun* 5:4797.
- 506 48. Lin W, Bazylinski DA, Xiao T, Wu L-F, Pan Y. 2014. Life with compass: diversity  
507 and biogeography of magnetotactic bacteria. *Environ Microbiol* 16:2646–2658.
- 508 49. Arakaki A, Takeyama H, Tanaka T, Matsunaga T. 2002. Cadmium recovery by a  
509 sulfate-reducing magnetotactic bacterium, *Desulfovibrio magneticus* RS-1, using  
510 magnetic separation. *Appl Biochem Biotechnol* 98–100:833–840.
- 511 50. Byrne ME, Ball DA, Guerquin-Kern J-L, Rouiller I, Wu T-D, Downing KH, Vali H,  
512 Komeili A. 2010. *Desulfovibrio magneticus* RS-1 contains an iron- and phosphorus-  
513 rich organelle distinct from its bullet-shaped magnetosomes. *Proc Natl Acad Sci U*  
514 *S A* 107:12263–12268.
- 515 51. Rousset M, Casalot L, Rapp-Giles BJ, Dermoun Z, de Philip P, Bélaich J-P, Wall  
516 JD. 1998. New Shuttle Vectors for the Introduction of Cloned DNA in *Desulfovibrio*.  
517 *Plasmid* 39:114–122.

518

519 **Figure 1.** Schematic of deletion methods used in *Desulfovibrio* spp. (A-C) Plasmids  
520 (dashed lines) are designed to replace a target gene (X, aqua arrow) in the  
521 chromosome (blue line) with a streptomycin resistance cassette (*strAB*, purple arrow).  
522 Regions upstream (\*) and downstream (\*\*\*) of the target gene (blue boxes) on the  
523 chromosome undergo recombination (red lines) with homologous regions that are  
524 cloned into the deletion plasmid. Key steps, such as recombination events (red  
525 crosses), are indicated in the boxes and the selection steps are labeled in red. (A)  
526 Double recombination can occur in one step after plasmids are linearized by

527 endogenous restriction enzymes. Mutants are selected using the marker (*e.g. strAB*)  
528 that was exchanged with the target gene. **(B)** Two-step double recombination is  
529 possible when suicide vectors integrate into the chromosome in the first homologous  
530 recombination event and then recombine out after the second homologous  
531 recombination event. The first step and second step are selected for with antibiotic  
532 resistance markers (*e.g. npt*) and counterselectable markers (*e.g. sacB*), respectively.  
533 **(C)** A replicative deletion plasmid designed to target genes for deletion may undergo  
534 double recombination in one or two steps as shown in A and B, respectively. After  
535 passaging the cells without antibiotic, mutants are selected with an antibiotic resistance  
536 cassette (*e.g. strAB*) and a counterselectable marker (*e.g. sacB*). *mob*, mobilization  
537 genes (*mobA'*, *mobB*, *mobC*) and *oriT*; *npt*, kanamycin-resistance gene; *ori<sub>Dm</sub>*, origin of  
538 replication for *D. magneticus*; *ori<sub>Ec</sub>*, origin of replication for *E. coli*.

539

540 **Figure 2.** Plasmids constructed for the present study. **(A)** Expression plasmid pAK914  
541 expresses *sacB* from the *mamA* promoter and is the parent vector for the deletion  
542 plasmids and *upp* expression plasmid described below. **(B)** Replicative deletion plasmid  
543 to target *upp* for markerless deletion. The *upp* deletion cassette was cloned into XbaI-  
544 SacI of pAK914. **(C)** Expression plasmid used for *upp* complementation. The *upp* gene  
545 and its promoter were cloned into BamHI-SacI of pAK914. **(D)** Replicative deletion  
546 plasmid to target *kupM* for marker exchange mutagenesis with *strAB*. The *kupM::strAB*  
547 deletion cassette was cloned into XbaI of pAK914. Labeling and colors correspond to  
548 Figure 1.

549



550 **Figure 3.** (A) The *upp* gene encodes UPRTase which is a key enzyme in the uracil  
551 salvage pathway. The product of the UPRTase reaction, UMP, is processed by  
552 downstream enzymes in pathways for RNA, DNA, and sugar nucleotide synthesis. 5-FU  
553 causes cell death by incorporating into this pathway via UPRTase. (B) Schematic of  
554 genomic region of *upp* in WT or  $\Delta$ MAI (top) and the  $\Delta$ *upp* mutant (bottom). (C) Genomic  
555 region of *kup* in WT (top) and *kup::strAB* (bottom). Primers used to screen for the  
556 correct genotype are indicated with half arrows. (D)  $\Delta$ *upp* mutants in WT and  $\Delta$ MAI  
557 backgrounds were confirmed by PCR using primers P19/P20 and agarose gel  
558 electrophoresis. WT and  $\Delta$ MAI show a band corresponding to the *upp* gene (2691 bp)  
559 while the  $\Delta$ *upp* mutants have a smaller band corresponding to a markerless deletion of  
560 the *upp* gene (2079 bp). The lower bands are likely non-specific PCR products. (E)  
561 *kupM::strAB* genotype confirmation by PCR and agarose gel electrophoresis using  
562 primers P21/P22 (WT=3069 bp; *kupM::strAB*=3263 bp,  $\Delta$ MAI=N/A).

563  
564 **Figure 4.** *upp* mutant and complementation phenotype. Growth of the parent strain  
565 ( $\Delta$ MAI) (A), *upp* deletion ( $\Delta$ MAI  $\Delta$ *upp*) (B), and complementation of the *upp* deletion  
566 ( $\Delta$ MAI  $\Delta$ *upp/upp*<sup>+</sup>) (C) when grown with 1.25  $\mu$ g/ml 5-FU (squares) or without 5-FU  
567 (circles). Data presented are averages from 2-3 independent cultures; error bars  
568 indicate the standard deviation.

569  
570 **Figure 5.** *kupM* mutant and complementation phenotype.  $C_{mag}$  values (A) and electron  
571 micrographs of WT (B), *kupM::strAB* (C), and  $\Delta$ *kupM::strAB/kup*<sup>+</sup> (D). Scale bars, 200

572 nm. Data presented are averages from 4 independent cultures; error bars indicate the  
573 standard deviation.

574

575 **TABLE 1.** Bacterial strains and plasmids used in this study.

Strain or plasmid	Genotype or relevant characteristics	Reference or source
Strains		
<i>E. coli</i>		
DH5α λpir	Cloning strain	Lab strain
WM3064	Conjugation strain; DAP auxotroph used for plasmid transfer	Lab strain
<i>D. magneticus</i>		
AK80	Non-motile mutant of <i>D. magneticus</i> strain RS-1, referred to as wild type	(50)
AK201	ΔMAI	(19)
AK267	ΔMAI Δupp	This study
AK268	Δupp	This study
AK270	ΔkupM::strAB	This study
Plasmids		
pBMK7	Conjugative vector with pBG1 and pMB1 replicons; Kan <sup>r</sup>	(51)
pBMC7	Conjugative vector with pBG1 and pMB1 replicons; Cm <sup>r</sup>	(51)
pBMS6	Cloning vector; source of strAB; Str <sup>r</sup>	(51)
pLR6	pBMK7 with P <sub>mamA</sub> in HindIII-SalI; source of P <sub>npI</sub> ; Kan <sup>r</sup>	(19)
pLR41	pLR6 with P <sub>mamA</sub> -kupM in SalI; Kan <sup>r</sup>	(19)
pAK0	Cloning vector, source of sacB; Kan <sup>r</sup>	(10)
pAK914	pLR6 with sacB in SalI-XbaI; Kan <sup>r</sup>	This study
pAK920	pBMC7 with P <sub>npL</sub> -strAB inserted into SacI site; Cm <sup>r</sup> Str <sup>r</sup>	This study
pAK941	pAK914 with cassette of 1064 bp upstream and 1057 bp downstream of kupM flanking P <sub>npL</sub> -strAB in XbaI; Kan <sup>r</sup> Str <sup>r</sup>	This study
pAK1126	pAK914 with cassette of 991 bp upstream and 1012 bp downstream of upp in XbaI-SacI; Kan <sup>r</sup>	This study
pAK1127	pAK914 with P <sub>upp</sub> -upp in BamHI-SacI; Kan <sup>r</sup>	This study

576

577 **TABLE 2.** Growth rates and generation times of the parent strain (ΔMAI), Δupp mutant,  
578 and upp complementation in trans with and without treatment with 5-FU.

Strain	growth rate (h <sup>-1</sup> )		generation time (h)	
	- 5-FU	+ 5-FU	- 5-FU	+ 5-FU
ΔMAI	0.077 ± 0.0017	N/A	9.1 ± 0.2	N/A
ΔMAI Δupp	0.079 ± 0.0017	0.070 ± 0.0040	8.8 ± 0.2	10.0 ± 0.6
ΔMAI Δupp/upp <sup>+</sup>	0.076 ± 0.0041	N/A	9.1 ± 0.5	N/A

579

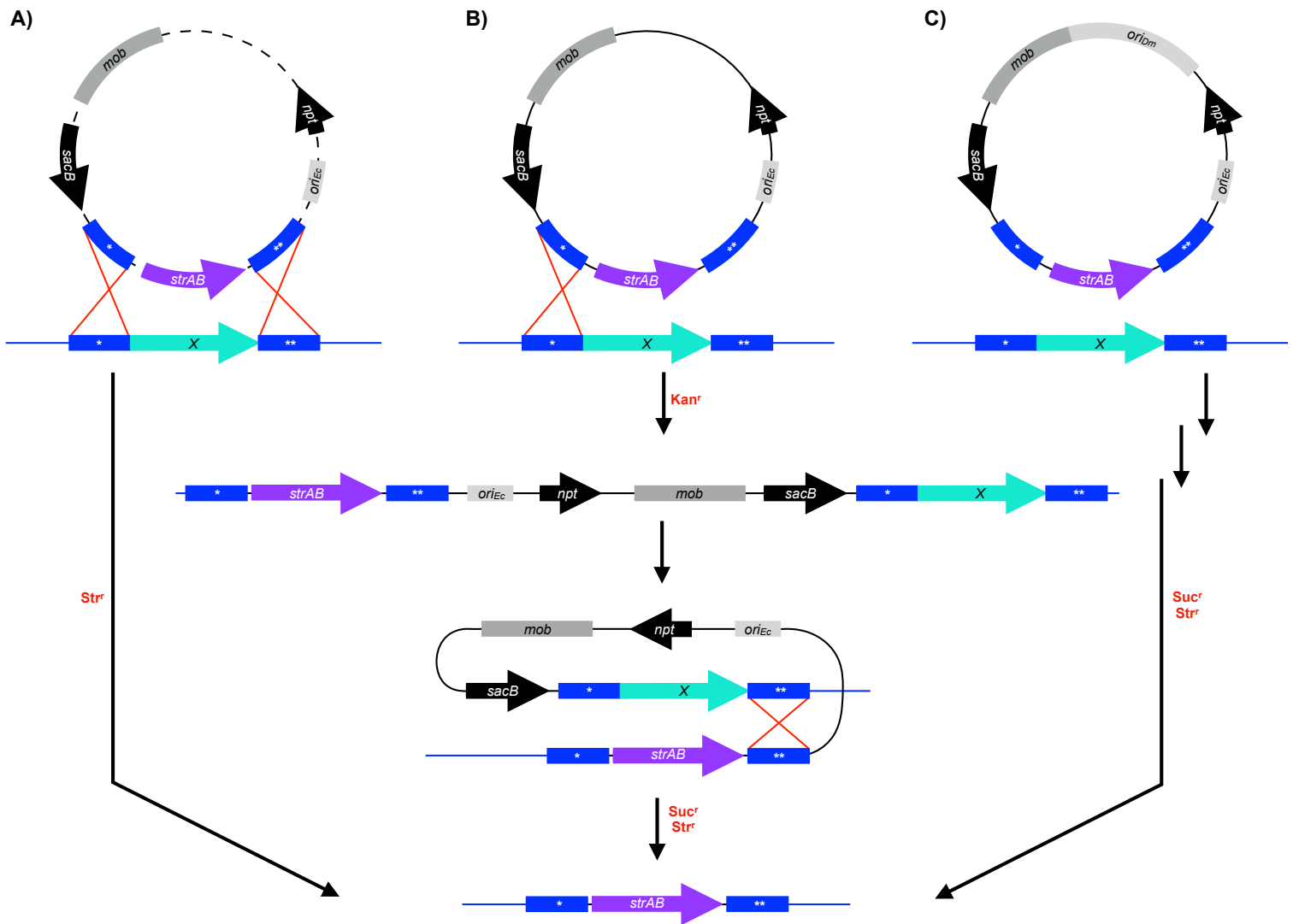


**Figure 1.** Schematic of deletion methods used in *Desulfovibrio* spp. **(A-C)** Plasmids (black lines) are designed to replace a target gene (X, aqua arrow) in the chromosome (blue line) with a streptomycin resistance cassette (*strAB*, purple arrow). Regions upstream (\*) and downstream (\*\*) of the target gene (blue boxes) on the chromosome undergo recombination (red lines) with homologous regions that are cloned into the deletion plasmid. Key steps, such as recombination events (red crosses), are indicated in the boxes and the selection steps are labeled in red. **(A)** Double recombination can occur in one step after plasmids are linearized (dashed lines) by endogenous restriction modification enzymes. Mutants are selected using the marker (e.g. *strAB*) that was exchanged with the target gene. **(B)** Two-step double recombination is possible when suicide vectors integrate into the chromosome in the first homologous recombination event and then recombine out after the second homologous recombination event. The first step and second step are selected for with antibiotic resistance markers (e.g. *npt*) and counterselectable markers (e.g. *sacB*), respectively. **(C)** A replicative deletion plasmid designed to target genes for deletion may undergo double recombination in one or two steps as shown in A and B, respectively. After passaging the cells without antibiotic, mutants are selected with an antibiotic resistance cassette (e.g. *strAB*) and a counterselectable marker (e.g. *sacB*). *mob*, mobilization genes (*mobA'*, *mobB*, *mobC*) and *oriT*; *npt*, kanamycin-resistance gene; *oriDm*, origin of replication for *D. magneticus*; *oriEc*, origin of replication for *E. coli*.

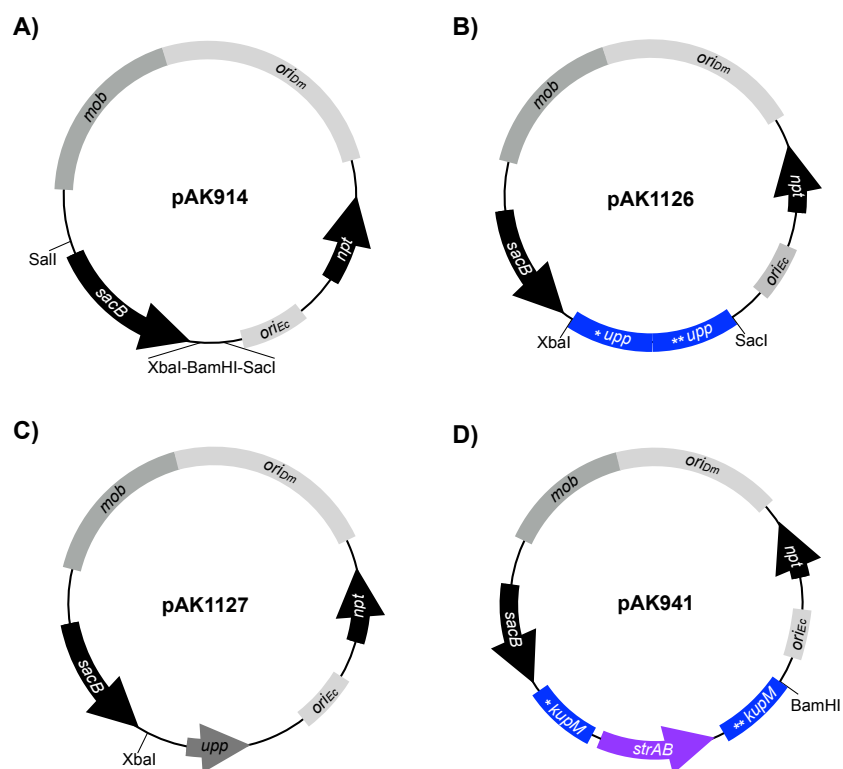


**Figure 2.** Plasmids constructed for the present study. **(A)** Expression plasmid pAK914 expresses *sacB* from the *mamA* promoter and is the parent vector for the deletion plasmids and *upp* expression plasmid described below. **(B)** Replicative deletion plasmid to target *upp* for markerless deletion. The *upp* deletion cassette was cloned into *XbaI*-*SacI* of pAK914. **(C)** Expression plasmid used for *upp* complementation. The *upp* gene and its promoter were cloned into *BamHI*-*SacI* of pAK914. **(D)** Replicative deletion plasmid to target *kupM* for marker exchange mutagenesis with *strAB*. The *kupM*::*strAB* deletion cassette was cloned into *XbaI* of pAK914. Labeling and colors correspond to Figure 1.

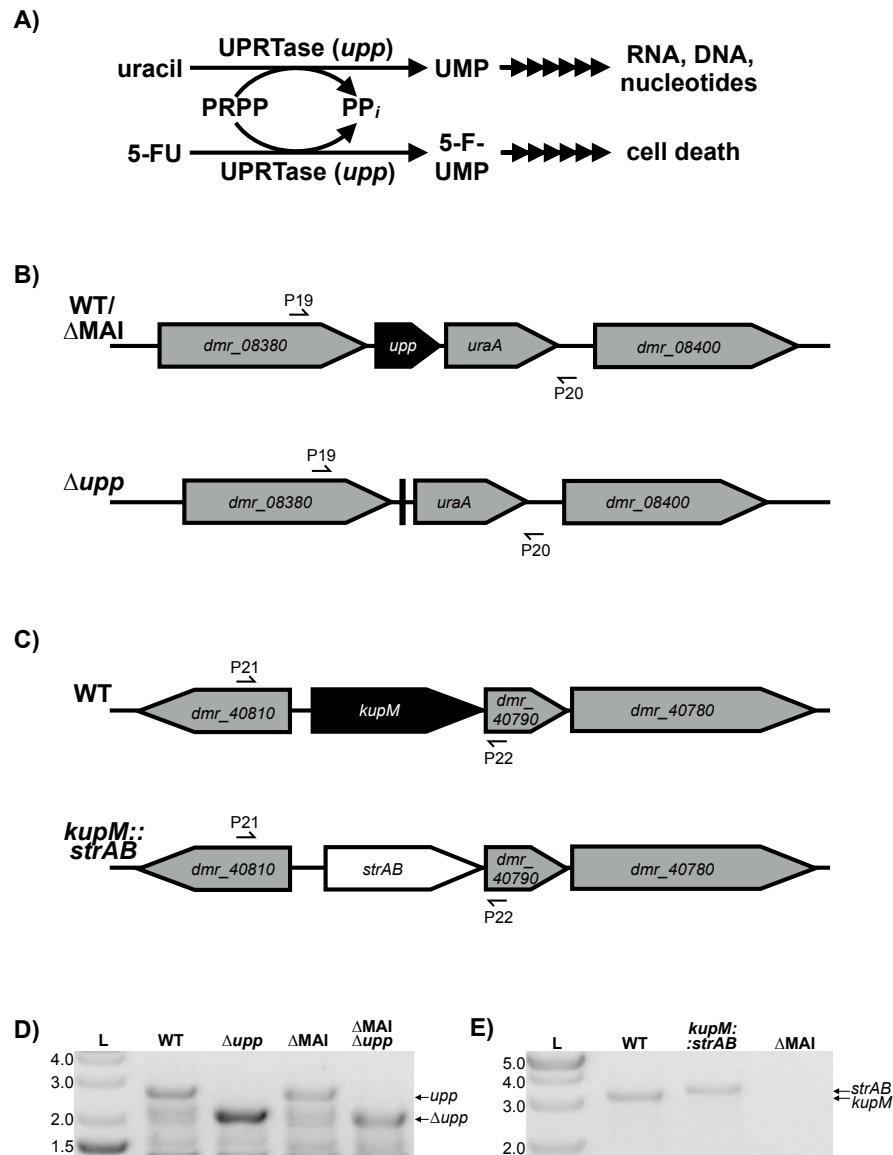


**Figure 3.** (A) The *upp* gene encodes UPRTase which is a key enzyme in the uracil salvage pathway. The product of the UPRTase reaction, UMP, is processed by downstream enzymes in pathways for RNA, DNA, and sugar nucleotide synthesis. 5-FU causes cell death by incorporating into this pathway via UPRTase. (B) Schematic of genomic region of *upp* in WT or  $\Delta$ MAI (top) and the  $\Delta$ *upp* mutant (bottom). (C) Genomic region of *kup* in wild-type (top) and *kupM::strAB* (bottom). Primers used to screen for the correct genotype are indicated with half arrows. (D)  $\Delta$ *upp* mutants in WT and  $\Delta$ MAI backgrounds were confirmed by PCR using primers P19/P20 and agarose gel electrophoresis. WT and  $\Delta$ MAI show a band corresponding to the *upp* gene (2691 bp) while the  $\Delta$ *upp* mutants have a smaller band corresponding to a markerless deletion of the *upp* gene (2079 bp). The lower bands are likely non-specific PCR products. (E) *kupM::strAB* genotype confirmation by PCR and agarose gel electrophoresis using primers P21/P22 (WT=3069 bp; *kupM::strAB*=3263 bp,  $\Delta$ MAI=N/A).

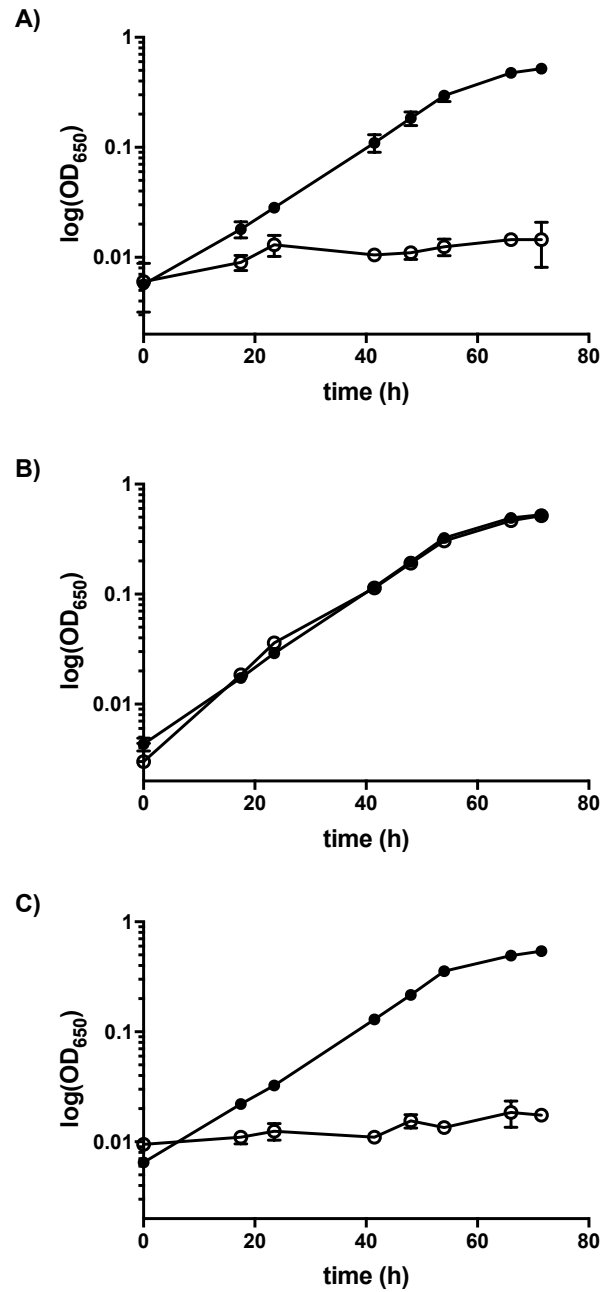


**Figure 4.** *upp* mutant and complementation phenotype. Growth of the parent strain ( $\Delta\text{MAI}$ ) (A), *upp* deletion ( $\Delta\text{MAI } \Delta\text{upp}$ ) (B), and complementation of the *upp* deletion ( $\Delta\text{MAI } \Delta\text{upp}/\text{upp}^+$ ) (C) when grown with 1.25  $\mu\text{g/mL}$  5-FU (squares) or without 5-FU (circles). Data presented are averages from 2-3 independent cultures; error bars indicate the standard deviation.

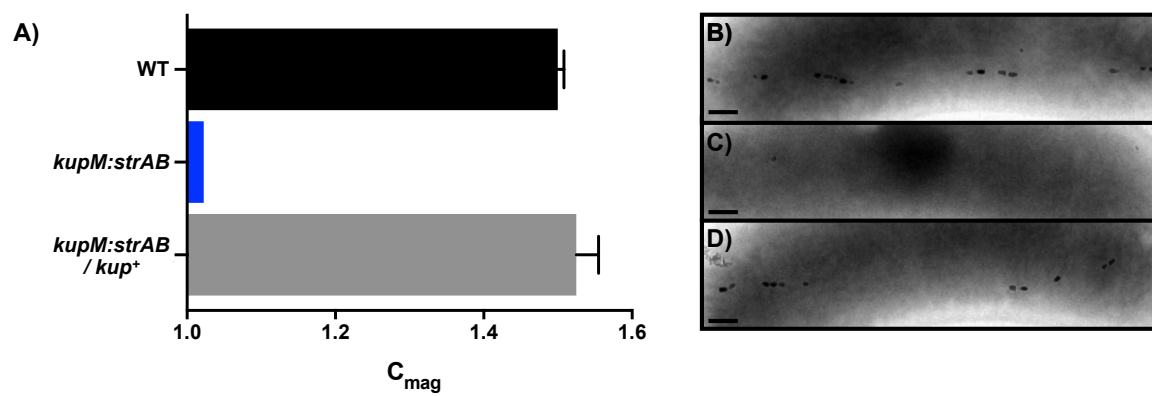


**Figure 5.** *kupM* mutant and complementation phenotype.  $C_{mag}$  values (A) and electron micrographs of WT (B), *kupM::strAB* (C), and  $\Delta kupM::strAB / kupM^+$  (D). Scale bars, 200 nm. Data presented are averages from 4 independent cultures; error bars indicate the standard deviation.